BL28B2
(White Beam X-ray Diffraction)

1. Introduction

BL28B2 is a bending magnet beamline that uses white X-ray beams from a bending magnet source without passing through a monochromator or other optical devices. This beamline is used in several research fields, including (1) X-ray diffraction, (2) dispersive-type time-resolved X-ray absorption fine structure (DXAFS), (3) microbeam radiation therapy (MRT), and (4) X-ray imaging. Therefore, various experiments such as biological functional imaging with small animals, fundamental research for radiation therapy, evaluation of structural materials using white X-ray diffraction and imaging, observations of dynamic structural changes during chemical reaction processes in catalysis and fuel cell batteries using time-resolved energy-dispersive XAFS, and three-dimensional observations of metallic objects using high-energy X-ray microtomography can be performed. To improve measurement techniques using this beamline, research and development of experimental techniques and instruments were conducted. The main activities in FY2018 are described below.

2. Beamline upgrades

2-1. X-ray diffraction: Introduction of new detector for white X-ray diffraction

In normal strain measurements and mineral identification in the region of interest inside the sample via energy-dispersive X-ray diffraction, X-ray CT is performed to understand the whole condition of a sample prior to the main measurement. As for the capability of the beamline, a sample with a diameter of several tens of millimeters can be measured using high-energy X-rays. However, CT images of thick samples could not be measured due to the narrow field of view of the detector. Therefore, a new camera was introduced (Fig. 1). The camera is an imaging unit M11427-62 from Hamamatsu Photonics with a field size of 28 mm. Hence, samples with a diameter of about 28 mm can now be evaluated.

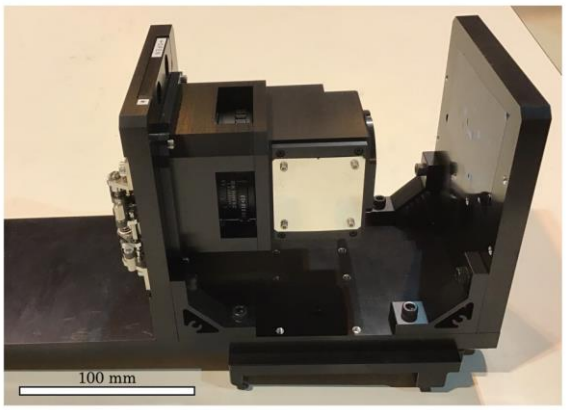

Fig. 1. New imaging unit M11427-62 from Hamamatsu Photonics.

2-2. DXAFS: Optimization of the phosphor screen for DXAFS detector

DXAFS is a powerful tool for local structure and chemical state analyses of materials during chemical reactions. In DXAFS measurements, the energy resolution and time resolution depend on the spatial resolution and X-ray sensitivity of the position-sensitive detector (PSD) for the detection of dispersed X-ray. The PSD used in the DXAFS station at BL28B2 is composed of a two-dimensional detector coupled with P43 (Gd_2O_2S: Tb^+) phosphor screen and a lens system. The spatial resolution and X-ray detection sensitivity of the detector depend on the particle diameter and

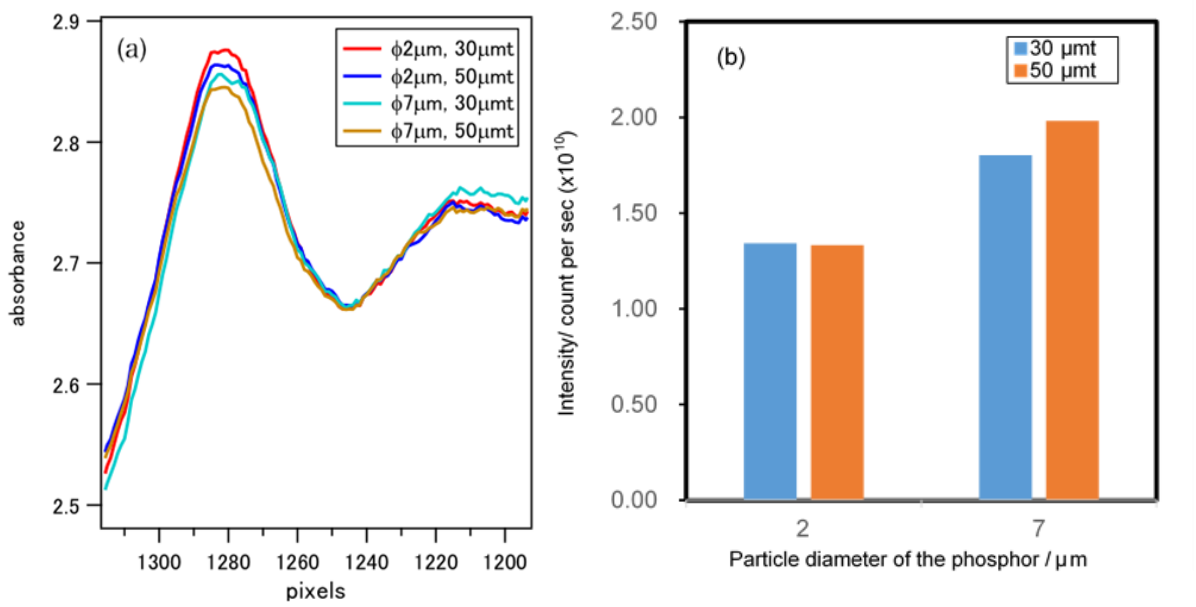

Fig. 2. (a) Fe K-edge DXANES spectra of Fe foil (horizontal axis is not converted to energy) and (b) the sensitivity of the detector.

thickness of the phosphor screen. To measure a wide energy range, in FY2018 we optimized the phosphor screen for the detector, which was developed in FY2016 [1].

Figure 2 shows a Fe K-edge (7.1 keV) DXANES spectra of Fe foil and the sensitivity of the detector when directly irradiated with an X-ray beam. As the particle diameter or thickness of the phosphor screen increases, the energy resolution decreases. On the other hand, the sensitivity of the detector increases with the particle diameter and a phosphor screen thickness in the range of 30–50 μm. In the future, we plan to upgrade the phosphor screen for DXAFS measurements in the high energy region.

2-3. Micro-CT: High-efficient and high-definition X-ray microtomography in the 200-keV region

A visible light conversion–type X-ray imaging detector with a tandem lens system is used for high-energy X-ray microtomography in the 200-keV region. This is because the extremely high penetration power of high-energy X-rays damages the imaging device in an in-line X-ray detector such as a direct imaging type X-ray camera. On the other hand, high-energy X-rays also penetrate a thin scintillator. Therefore, optimization of the scintillator is an important issue to improve the measurement efficiency. In previous measurements, a 20-μm-thick P43 powder scintillator was used where the photoelectric absorption by the scintillator was less than 0.5% at 200 keV [2]. In FY2018, a 500-μm-thick $Lu_3Al_5O_{12}:Ce^+$ (LuAG) single-crystal scintillator was introduced. Using a thick scintillator, the exposure and total measurement times are reduced to approximately 1/7 of that in the previous measurements.

To evaluate the spatial resolution when using a thick scintillator, the modulation transfer function (MTF) was measured using a test chart (Type-14 Moriyama X-ray Equipment). Figure 3 shows the measured MTFs. Although the image contrast in LuAG is

lower than that in P43 in the lower frequency region, almost the same spatial resolution is obtained in the thick scintillator. Additionally, a high-definition CMOS camera was introduced. Since the effective field of view can be defined by the effective pixel size and the number of pixels, the high-definition camera makes it possible to measure samples with a higher spatial resolution while maintaining a wide field of view. By combining the single-crystal scintillator with the high-definition camera, the throughput of raw data is increased approximately ten times compared with that in FY2017.

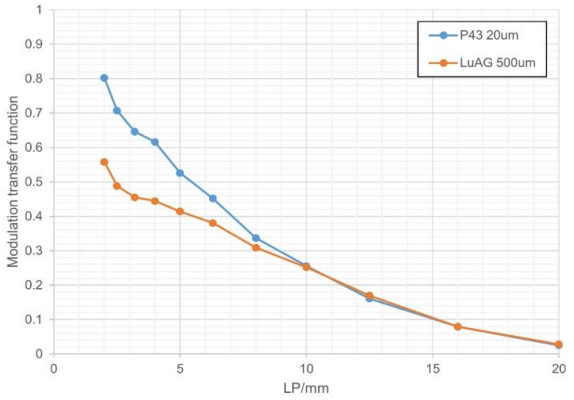

Fig. 3. Modulation transfer function measured when using a 500-μm-thick LuAG single-crystal scintillator and a 20-μm-thick P43 powder scintillator. Effective pixel size is 16 μm.

As a demonstration of highly efficient and high-definition X-ray microtomography, a limestone larger than 20 mm was measured with an effective pixel size of 2.36 μm. Figure 4 shows a sectional image of the limestone. A detailed structure of the inclusion is clearly observed. In the future, large field of view measurements for fossil samples, which are promising candidates for high-energy X-ray microtomography applications, as well as feasibility studies on the high-energy X-ray microtomography with a higher spatial resolution, will be considered.

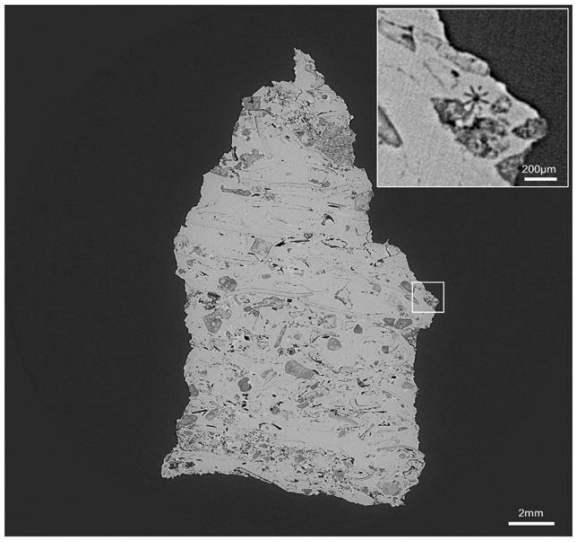

Fig. 4. Sectional image of a limestone measured with an effective pixel size of 2.36 μm. Effective field of view is 24.9 mm × 24.9 mm (10,549 × 10,549 pixels).

Masato Hoshino[*1], Keiji Umetani[*1], Kazuo Kato[*1], and Kentaro Kajiwara[*2]

[*1] Spectroscopy and Imaging Division, Center for Synchrotron Radiation Research, JASRI

[*2] Industrial Application Division, Diffraction and Scattering Division, JASRI

References:

[1] SPring-8/SACLA Annual Report, 2016, p65.

[2] M. Hoshino et al., *AIP Advances* **7**, 105122 (2017).